Active Site Analysis of the Potential Antimicrobial Target Aspartate Semialdehyde Dehydrogenase

Andrea Hadfield,*[,‡,§] Camille Shammas,[‡] Gitay Kryger,[§,⊥] Dagmar Ringe,[§] Gregory A. Petsko,[§] Jun Ouyang,[#,||] and Ronald E. Viola[#]

Department of Biochemistry, School of Medical Sciences, University of Bristol, University Walk, Bristol BS8 1TD, England, Department of Biochemistry, Rosenstiel Basic Medical Sciences Research Center, Brandeis University, Waltham, Massachusetts 02254-9110, and Department of Chemistry, University of Toledo, Toledo, Ohio 43606

Received August 22, 2001; Revised Manuscript Received October 5, 2001

ABSTRACT: Aspartate-β-semialdehyde dehydrogenase (ASADH) lies at the first branch point in the biosynthetic pathway through which bacteria, fungi, and the higher plants synthesize amino acids, including lysine and methionine and the cell wall component diaminopimelate from aspartate. Blocks in this biosynthetic pathway, which is absent in mammals, are lethal, and inhibitors of ASADH may therefore serve as useful antibacterial, fungicidal, or herbicidal agents. We have determined the structure of ASADH from *Escherichia coli* by crystallography in the presence of its coenzyme and a substrate analogue that acts as a covalent inhibitor. This structure is comparable to that of the covalent intermediate that forms during the reaction catalyzed by ASADH. The key catalytic residues are confirmed as cysteine 135, which is covalently linked to the intermediate during the reaction, and histidine 274, which acts as an acid/base catalyst. The substrate and coenzyme binding residues are also identified, and these active site residues are conserved throughout all of the ASADH sequences. Comparison of the previously determined apoenzyme structure [Hadfield et al. *J. Mol. Biol*. (1999) *289*, 991−1002] and the complex presented here reveals a conformational change that occurs on binding of NADP that creates a binding site for the amino acid substrate. These results provide a structural explanation for the preferred order of substrate binding that is observed kinetically.

Aspartate β-semialdehyde dehydrogenase (ASADH, EC 1.2.1.11)[1] is an essential enzyme found in bacteria, fungi, and higher plants (*1*). This NADP-dependent enzyme catalyses the reductive dephosphorylation of aspartyl β-phosphate to aspartate β-semialdehyde as the second step in the common biosynthetic pathway. From here the pathway branches, and the aspartate β-semialdehyde can either be further reduced to homoserine, which leads to methionine, threonine, or isoleucine, or it can be condensed with pyruvate and cyclized into dihydrodipicolinate, and then converted into diaminopimelate (DAP), a component of bacterial cell walls, and finally decarboxylated to produce lysine (Figure 1). Inhibition of the biosynthesis of these essential products is a possible strategy for the development of novel antibiotic, fungicidal, or herbicidal compounds. Blocks in this biosynthetic pathway are lethal, as demonstrated by the successful production of vaccines for *Salmonella typhimurium* (*2*) and *Streptococcus mutans* (*3*) using strains with mutations in the *asd* gene that encodes for ASADH. This is largely because of the role that this pathway plays in the production of DAP, a crucial component for the cross-linking of bacterial cell walls. On the other hand, mammals are deficient in lysine biosynthesis and therefore require a dietary source of this amino acid. Thus, there is interest in enhancing lysine yields in crop plants through an improved understanding of the regulation of the biosynthetic pathway leading to its production.

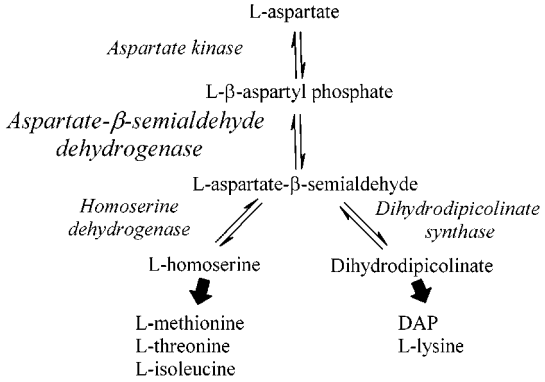

FIGURE 1: The biosynthetic pathway leading from aspartate to the essential amino acids lysine, threonine, isoleucine, and methionine, and also the bacterial cell wall cross-linking agent diaminopimelate.

* To whom correspondence should be addressed. Department of Biochemistry, School of Medical Sciences, University of Bristol, University Walk, Bristol BS8 1TD, England. Telephone: 0117 928 8593. E-mail: a.t.hadfield@bris.ac.uk.

[‡] University of Bristol.

[§] Brandeis University.

[#] University of Toledo.

[⊥] Current address: Computational Chemistry and Drug Design, Compugen Ltd., 72 Pinchas Rozen Street, Tel-Aviv 69512, Israel.

[||] Current address: Bayer Corp., Berkeley, California.

[1] Abbreviations: ASADH, aspartate β-semialdehyde dehydrogenase; ASA, aspartate β-semialdehyde; DAP, diaminopimelate; *E. coli*, *Escherichia coli*; GAPDH, glyceraldehyde 3-phosphate dehydrogenase; NAD, nicotinamide adenine dinucleotide; NADP(H), nicotinamide adenine dinucleotide phosphate; SMCS, *S*-methyl cysteine sulfoxide.

10.1021/bi015713o CCC: $20.00
Published on Web 11/08/2001

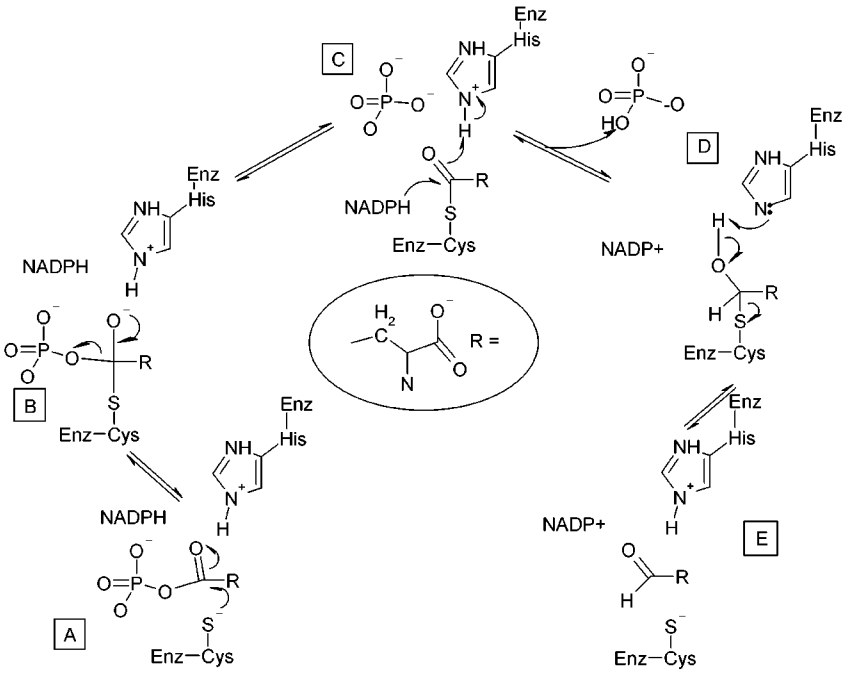

FIGURE 2: The chemical mechanism of catalysis of the conversion of aspartyl β-phosphate to aspartate semialdehyde by ASADH.

Over 70 gene sequences encoding aspartate semialdehyde dehydrogenase from different organisms have now been deposited in the protein database SWISSPROT, and sequence alignments indicate a wide range of overall sequence identity. Early studies on the enzyme (*4*, *5*) indicated that the catalytic mechanism was likely to be similar to that of the ubiquitous enzyme glyceraldehyde-3-phosphate dehydrogenase (GAPDH). In the biosynthetic direction, ASADH forms L-aspartate-β-semialdehyde by the reductive dephosphorylation of L-β-aspartyl phosphate utilizing NADPH. A chemical mechanism has been proposed (*6*), based on pH and chemical modification studies, and the catalytic base subsequently identified in the crystal structure of the apo-enzyme (*7*) (Figure 2).

The proximity of an active site base generates the cysteine thiolate nucleophile that attacks the carbonyl carbon of β-aspartyl phosphate to form a tetrahedral intermediate (B). Collapse of this intermediate with expulsion of phosphate results in the formation of a stable thioacyl-enzyme intermediate (C). Hydride transfer to this intermediate from NADPH forms a second tetrahedral intermediate (D), with subsequent collapse via expulsion of the cysteine thiolate to produce aspartate β-semialdehyde (E). Kinetic analysis shows that the mechanism has a preferred but not obligatory binding order, with aspartyl phosphate binding to the E-NADPH complex, and ordered release of the products ASA and NADP. A similar mechanism has been proposed for GAPDH (*8*) with an equivalent role for a cysteine thiolate, and a histidine residue acting as a general base catalyst for hydride transfer.

In *E. coli*, ASADH is active as a homodimer with a subunit molecular mass of 39 kDa. We have recently solved the structure of ASADH from *E. coli* (*7*), in the apo form. Here we report the structure in the presence of NADP and a substrate analogue, *S*-methyl cysteine sulfoxide (SMCS), which binds covalently to the enzyme. Examination of this ternary complex has allowed the identification of the key catalytic and binding groups of ASADH. This knowledge of the binding interactions of the substrate analogue will be useful in design of potential antimicrobial compounds.

Table 1: Crystallographic Structure Solution and Refinement

data collection	
unit cell dimensions ($P6_4$)	$a = b = 121.0$, $c = 94.0$ Å, $\alpha = \beta = 90°$, $\gamma = 120°$
V_M (Å^3 D^{-1}), solvent content	2.75, 55%
unique reflections (redundancy)	22099 (1.9)
R_{sym} (outer shell, 2.6−2.74 Å) %	10.3 (30.7)
completeness (outer shell, 2.6−2.74 Å) %	96.3 (61.6)
refinement	
data range (all data with $F > 0.0$)	28.0−2.6 Å
no. refl. in work set (test set)	21181 (918)
R factor (R_{free})	20 (26.2)
rms dev. from ideality: bonds (Å), angles	0.006, 1.32
⟨B-factor⟩	28.3

MATERIALS AND METHODS

Crystallization, Data Collection, and Processing. The enzyme was overexpressed and purified as reported (*6*, *9*, *10*). The enzyme stock used for crystallization was concentrated to 10 mg/mL using centricons (Amicon) and dialyzed against a buffer with 10 mM HEPES, 1 mM DTT, 1 mM EDTA, and 1 mM NaN_3 at pH 7.0. Crystals of ASADH were grown at 4 °C by the hanging drop method, adding equal volumes of the enzyme stock solution and a reservoir solution comprising 19% PEG 4 K, 0.35 M $MgCl_2$, 0.2 M ammonium acetate in a 0.1 M acetate buffer at pH 4.6. 5 mM NADP and 2 mM SMCS were present in the enzyme stock solution. Crystals grew in space group $P6_4$, with unit cell dimensions $a = b = 121.0$, $c = 94.0$ Å and one dimer in the asymmetric unit. Data were collected at 100 K on a rotating anode generator, recording 0.3 degrees of data per image using MAR image plates and was reduced using the XDS package. The CCP4 suite (*11*) was used for scaling and all subsequent processing (Table 1).

Structure Solution and Refinement. The structure was solved by molecular replacement using the program AMORE. A dimer of the apo enzyme was taken as the search model,

and this approach located a dimer in the asymmetric unit using data from 10 to 4 Å resolution and a sphere of integration of 30 Å.

A set of reflections (5%) was set aside from the beginning for validation of the model building and refinement process using R_{free} (*12*). Model building was performed using the program O (*13*). The model was refined using the program XPLOR (*14*) (Table 1), using iterative cycles of simulated annealing refinement, model building, and, for the first few iterations, electron density averaging using the Uppsala suite of averaging programs (*15*). Strict noncrystallographic symmetry was used for refinement until no further improvement could be made. The constraints were then relaxed to restraints, which reduced the R_{free} value. Omit maps were calculated (15 residues at a time) along the length of both protein chains to guide the release of restraints in some parts of the structure. The final model was refined using all data from 28.0 to 2.6 Å and contains 734 amino acid residues (5620 protein atoms), one covalent ligand (7 atoms), two NADP molecules (96 atoms), and 171 water molecules. In the final model, 87.3% of the residues (*16*) lie in the most favored regions of a Ramachandran plot (*17*), while no residues lie outside the additionally allowed regions. However residue 355, a conserved alanine that lies between the domains (the putative hinge region), lies right on the boundary between the additionally and generously allowed regions for a right-handed α-helix. The refined coordinates have been deposited with the PDB and assigned the entry code 1gl3.pdb.

RESULTS

Structure Description. The N-terminal domain of ASADH is an approximate Rossmann fold that provides the binding site for NADP, while the C-terminal domain is responsible for dimerization, for binding of ASA, and for providing the catalytic residues. The structure reported here is a dimer, which has NADP and a covalent ligand bound in one subunit and NADP alone in the other subunit (Figure 3). The overall structure of the two subunits is very similar, and the following discussion will refer to both subunits unless otherwise stated.

There are two major structural differences between the apo structure previously published (*7*) and the substrate complex reported here. There is a change in the relative position of the two domains, which can be described as a domain closure with rotation of the NADP binding (N-terminal) domain toward the dimerization (C-terminal) domain of approximately 6° about X (Figure 3B). This rotation results in the cleft between the two domains closing up around the NADP. The Cα positions of residues close to the active site are displaced by around 1.5 Å relative to their position in the apo enzyme, whereas the displacement is as much as 5 Å at the far end of the Rossmann fold where the 3′ phosphate of the NADP binds. Second, a loop from Asp 231 to Glu 242 that is disordered in the apo structure becomes ordered in the ternary complex (Figure 3C). The driving force for this loop ordering is the formation of new hydrogen bonds that are observed in the holo structure between residues that are too far apart to form hydrogen bonds in the "open" conformation observed in the apo structure. The side chain hydroxyl of Ser 99 forms a new hydrogen bond with the side chain of Arg 240. The side chain of Asn 134 forms hydrogen bonds with the side chains of Glu 241 and possibly Lys 244. The repositioning of Asn 134 is stabilized by a water-mediated hydrogen bond between Asn 134 and Arg 102. There is also a water-mediated hydrogen bond between Lys 244 and the 2′ hydroxyl of the nicotinamide sugar moiety. These hydrogen bonds are all possible as a result of the domain shift, and these new interactions stabilize the protein structure in the vicinity of the active site loop that has become ordered. These interactions are observed in both subunits, so neither the domain rotation nor the loop closure appears to be dependent on the presence of the amino acid substrate.

Active Site and Catalysis. Inhibitor Modifies Catalytic Cysteine. The location of the active site has previously been identified through the presence of the catalytic cysteine, Cys 135, which was assigned by site-directed mutagenesis studies (*18*). The covalent attachment of the inhibitor to Cys 135 in subunit A further confirms this residue as the catalytic cysteine. The inhibitor *S*-methyl cysteine sulfoxide, an analogue of aspartate-β-semialdehyde, was present at all times during crystallization, and the observed density is consistent with disulfide bond formation between the inhibitor, which is therefore an inactivator for this enzyme, and the active site cysteine (Figure 4). However, there is no electron density for either a methyl or a sulfoxide substituent on the sulfur, which is therefore modeled as cystine. The mechanism of the attack and subsequent reaction between the active site cysteine and SMCS has not been established. Omit maps calculated by omitting the active site cysteine and other residues with any atom within 3.5 Å confirms the presence of SMCS in the A site and only solvent in this position in the B site (Figure 4C,D). Mass spectrometry also confirms the presence of a covalent adduct, with an approximate mass of 120 Da corresponding to the weight of cysteine, in roughly 50% of the active sites (unpublished data).

Conserved Residues Identified in Binding of Substrate Analogue. Figure 4 shows a schematic of the residues interacting with the substrate analogue. The α-amino group is within hydrogen bonding distance of both Gln 162 and Glu 241. Gln 162 is conserved throughout the sequences currently available, while Glu 241 lies on the active site loop that is disordered in the apo structure. Arg 267, which is also fully conserved, forms an electrostatic interaction with the substrate carboxyl group. The substrate analogue differs from the substrate only at the gamma position in the side chain, so these interactions would presumably also be observed with the natural substrate, aspartate semialdehyde.

Comparison of A and B Subunits: with and without Inhibitor. Most of the protein was refined subject to strict crystallographic constraints to maintain the ratio of data to refined parameters as high as possible. However, these constraints were relaxed to restraints in the final rounds of refinement and restraints were removed in parts of the structure where the electron density clearly showed differences between the subunits. These differences are generally on the surface of the protein where crystal contacts are not the same for both subunits. Restraints were also removed on the ASA binding residues since SMCS was only found in subunit A. Despite this, there was no measurable difference in conformation of the substrate binding residues. The position of NADP is slightly different in the two subunits,

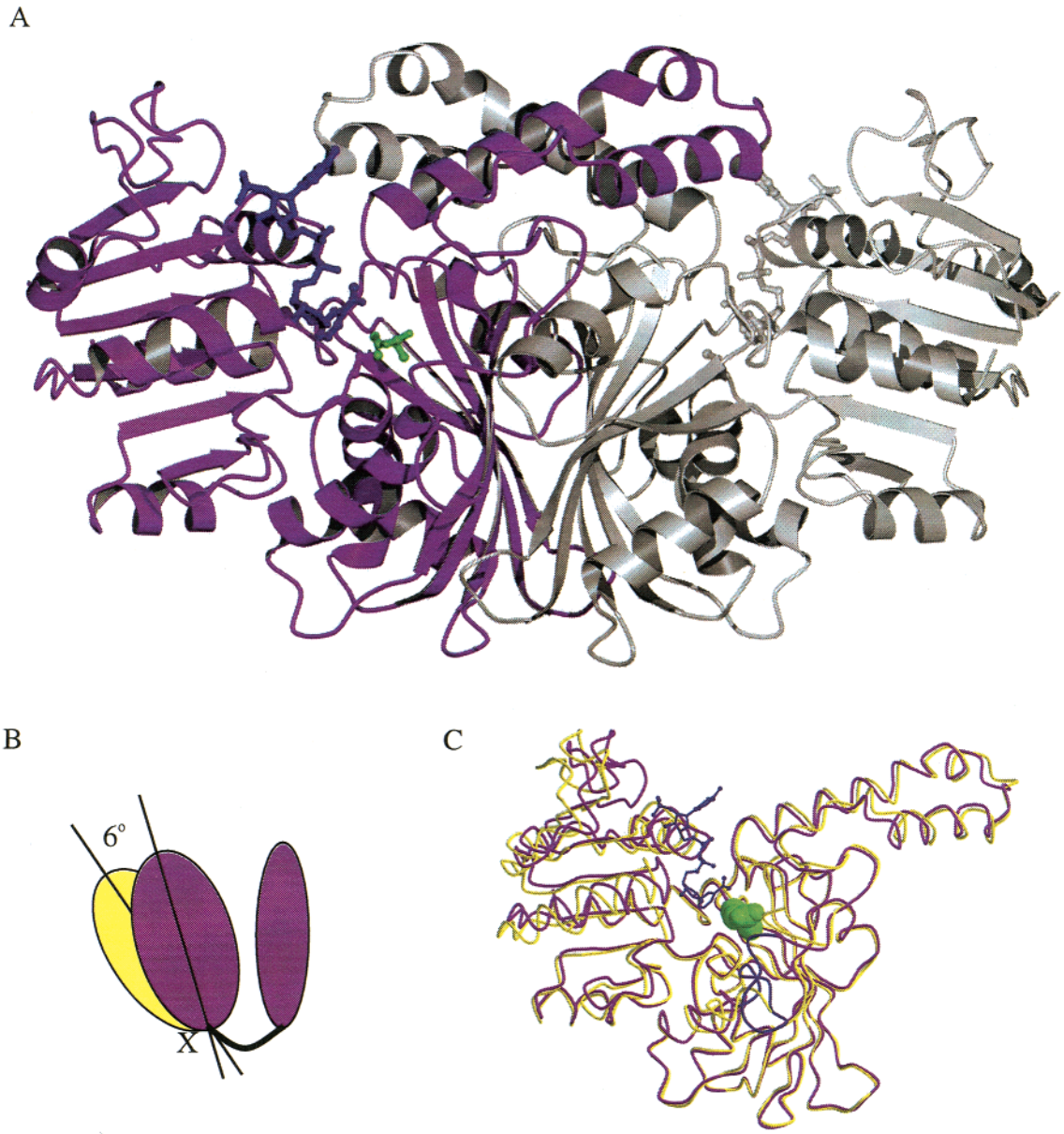

FIGURE 3: (A) Ribbon diagram of the ASADH dimer, with the ligands NADP (blue) and SMCS (green) shown by ball-and-stick representation. Subunit A is colored magenta. (B) Cartoon of domain closure. The two domains of subunit A of the holo enzyme are represented in magenta, in the same orientation as panel A. The two domains of subunit A of the apo enzyme are represented in yellow. X marks the position of the point about which the N-terminal domain of subunit rotates. (C) Superposition of C_α traces of the apo (yellow) and holo (magenta) monomers in the same orientation as panel A. NADP (shown in ball-and-stick representation) and the loop that becomes ordered upon binding of NADP are shown in blue. The SMCS is shown in space-filling representation and is colored green.

with NADP being displaced a bit more than 0.5 Å toward the catalytic cysteine in the unoccupied active site. Non-crystallographic symmetry operators or restraints were applied separately for the two domains from early in the refinement, which resulted in better improvement in the free R-factor. This lends validity to the small systematic displacement observed between the N-terminal domain in subunits A and B, which corresponds to the B subunit being slightly more "open", with a displacement of Cα residues at the most extreme point around residue B40 of 1 Å (as compared to a maximum displacement of 5 Å in the apo "open" structure).

There are four areas of crystal contacts. Two are across crystallographic 2-fold axes. At the N-terminus, residues A1−A2 packs against residues B1−B2 of a symmetry related molecule and vice versa. Along the bottom of the molecule as shown in Figure 3, loop A103−A105 packs against loop B234−B237 of a symmetry related molecule, and loop B235−B237 packs against loop A103-A105 of the same symmetry related molecule. The other two areas of contact are more revealing since they reflect the observed asymmetry of the dimer. One symmetry related molecule is arranged so that helix F, the first helix in the "arm" subdomain, slots into the top of the active site cleft in the A subunit (the helical axis would be perpendicular to the page in Figure 3). There is a crystal contact between Arg 10 in the A subunit at the top of the active site cleft, where the adenine moiety binds, and Asp 188 in the A subunit of the symmetry related molecule. There is no equivalent interaction with the top of the active site cleft in subunit B. A separate symmetry molecule lies along the top edge of domain 1 in subunit B, with the backbone of Ala 43 making a hydrogen bond with Gly 211 in the A subunit of the symmetry molecule.

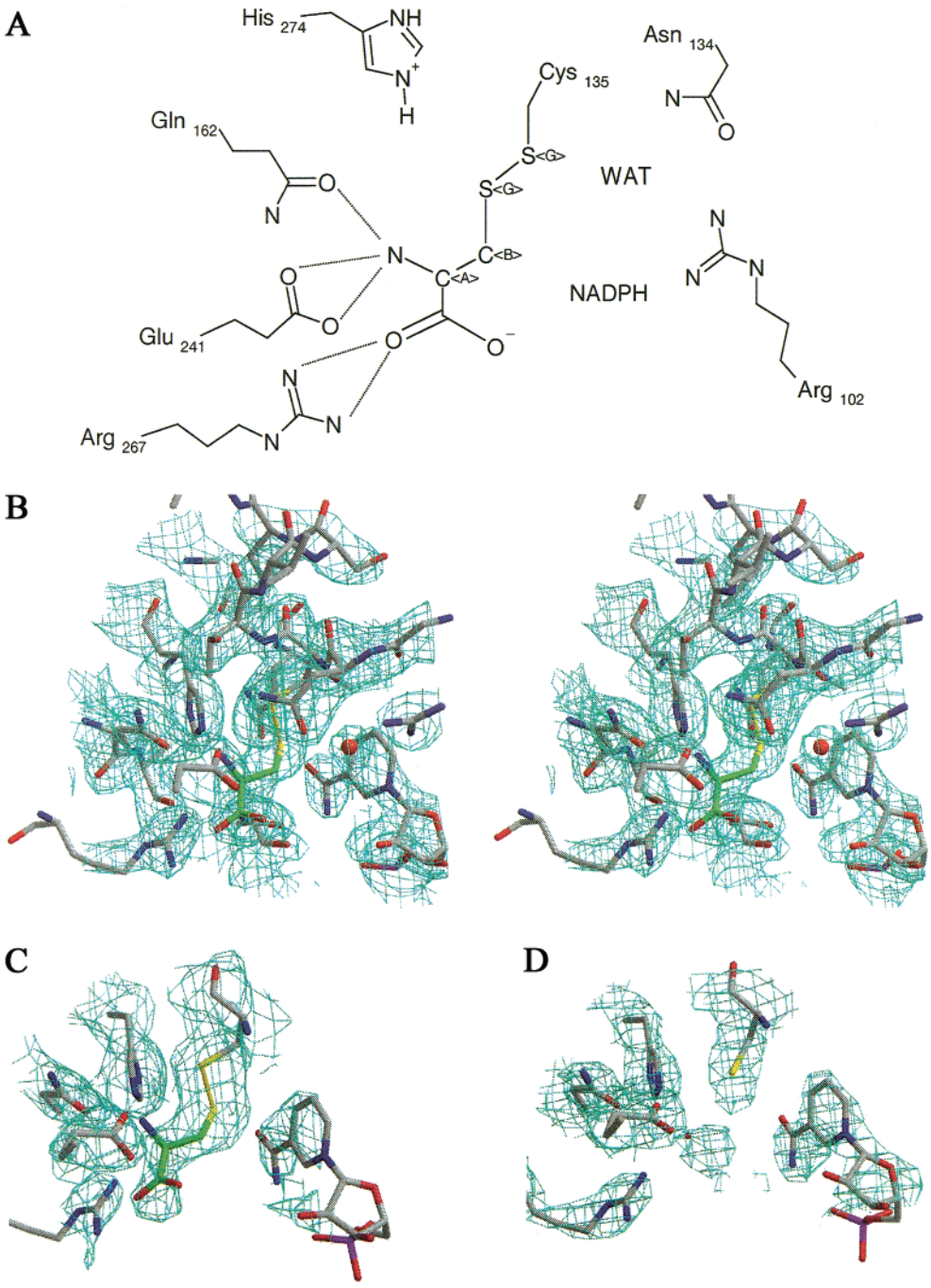

FIGURE 4: (A) Schematic drawing of residues interacting with the visible portion of SMCS (cysteine) in the active site. (B) Stereo diagram showing 2*F*o−*F*c density contoured at 1.3 sigma in the A subunit active site. (C and D) Electron density in the A subunit and B subunit active sites calculated after omitting from the model the catalytic cysteine 135 and residues with any atom within 3.5 Å.

NADP Binding. The dinucleotide NADP binds similarly in subunit A and subunit B, and its binding appears to be responsible for the conformational change between the "open" apo form and the "closed" holo form of the enzyme. Once the NADP has bound, the altered conformation of the protein at the active site is ready to accept substrate with very little change required even in side chain positions. Despite the slight differences in the refined positions of the NADP in each monomer mentioned above, NADP makes the same interactions with the enzyme in both subunits. There are also slight differences in conformation at the end of the "arm" subdomain where one subunit interacts with the adenine base of the NADP bound in the opposite subunit. However, at the resolution limits in the current structure these differences are too small to be meaningfully interpreted.

The nitrogen of the nicotinamide amide is within hydrogen bonding distance of the mainchain carbonyl oxygen of residues Ser 165 and Gly 166 and its own phosphate group (Figure 5). The carbonyl oxygen of the nicotinamide amide is within hydrogen bonding distance of Gln 350, and a glutamine or asparagine is seen in all of the ASADH sequences in this position. These interactions with the nicotinamide amide group give ASADH its stereospecificity as a class B (pro-R) dehydrogenase. On the nicotinamide sugar moiety OH1 hydrogen bonds with the mainchain amide from Gly 75, while OH2 makes the water mediated hydrogen

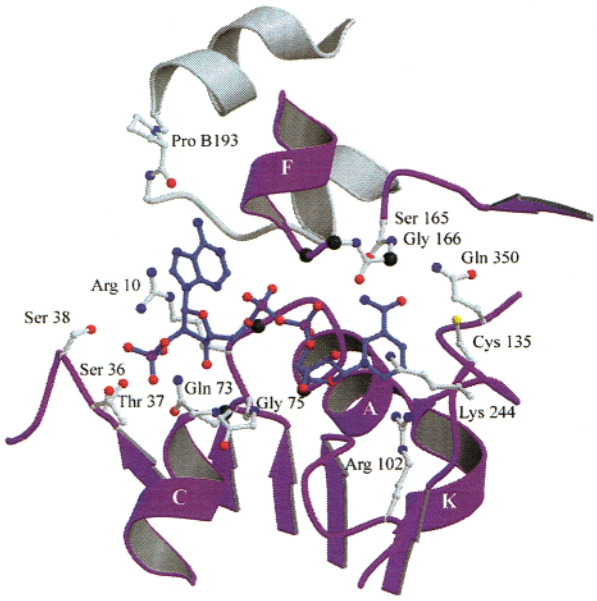

FIGURE 5: The interactions made between enzyme residues and NADP. Protein is shown in cartoon representation, with interacting residues shown in ball-and-stick representation.

bond with Lys 244 already mentioned in the context of conformational change.

The nicotinamide phosphate lies at the N terminus of helix A and forms hydrogen bonds with the mainchain nitrogen of Met 12, Val 13, and Gly 168. The adenine phosphate lies within hydrogen bonding distance with the mainchain nitrogens of Met 12 and Ala 169. It is positioned between the N termini of helix C in the Rossmann fold domain and helix F in the dimerization domain. The loop from 163 to 168 is highly conserved among the ASADHs, with a consensus sequence S/A x S G S/A/G G, where x is a small hydrophobic residue (A,V,L). This loop with small side chains allows mainchain hydrogen bonding with both the nicotinamide and the bridging pyrophosphate in NADP and provides one side of a well-fitting cleft for the NADP. It therefore has a similar role to the loop on the Rossmann fold bearing the traditional hallmark of NAD(P) binding, the sequence motif G x G xx G.

The adenine-half of the dinucleotide makes a number of interactions with both domains of one subunit. The 3′ phosphate on the adenine sugar moiety lies within hydrogen bonding distance of the side chains of Arg 10, Ser 36, Thr 37, Ser 38, and Gln 73. Arg 10 also stacks against the adenine base, which in turn is hydrogen bonded to the carbonyl oxygen of Pro 193 from the tip of the "arm" subdomain of the opposite subunit.

DISCUSSION

Mechanistic Implications. The structures presented here shed light on a number of features of the catalytic reaction cycle (Figure 2). The previously determined structure (*7*) represents the apo enzyme. Subunit B of the present structure represents the E-NADP product complex (structure E) in the chemical mechanism (Figure 2) and suggests that upon binding of NADP a domain closure takes place, which in turn promotes the stabilization of the protein mainchain between residues 231 and 242. The binding of NADP (and also presumably the binding of NADPH) creates a binding pocket for the substrate, aspartyl phosphate, or ASA that is not present in the apo structure. These observations are consistent with kinetic analysis that shows that the mechanism has a preferred binding order, with NADPH binding before aspartyl phosphate and with NADP and phosphate binding before the substrate aspartate semialdehyde in the reverse reaction. In subunit A, where *S*-methyl cysteine sulfoxide binds covalently to the catalytic cysteine, the active site structure resembles a complex with the hemiacetal or thioester intermediate (Figure 2, structure C) in the chemical mechanism.

Catalysis. The sulfur Sγ of SMCS corresponds to the carbonyl carbon of the substrate which accepts/donates a hydride from/to NADP(H) during catalysis. The spatial arrangement of SMCS relative to the NADP is consistent with it binding to the enzyme as an intermediate analogue. Although the distance between this sulfur and carbon-4 of NADP is somewhat long at 3.5 Å, it is expected to be shorter during hydride transfer to the true substrate. The mechanism proposes that an enzymic base facilitates nucleophilic attack by the cysteine thiolate anion on the carbonyl carbon. The proposed role of His 274 as this acid/base catalyst (*7*) is strongly supported by the current structure. Nϵ of the imidazole lies 3.6 Å from Sγ of SMCS. In the substrate, an oxygen would be positioned between Cγ, represented by Sγ in SMCS and the histidine. It is this oxygen that would be protonated by the histidine or have a proton removed. His 274 therefore lies in an appropriate position for this role. The average pK_a of a histidine residue is also suited to the role as an acid/base catalyst. During the reaction, a positive charge develops on the histidine at two stages. There are two residues that are located just beyond hydrogen bonding distance in the current structure that, with small changes in conformation, could stabilize the developing positive charge, Gln 350 on one side and Gln 162 on other side. Gln 162 is completely conserved in ASADH, and a glutamine or asparagine is always observed in the other position. Mutational studies were performed prior to the structure determination (*19*) where Gln 162 was replaced by an asparagine and a histidine. The K_M for ASA was not changed significantly in either of these mutants, whereas the k_{cat} was reduced 13-fold by the Asn substitution and 3-fold by the histidine substitution. These structural studies suggest two possible interpretations of the mutational results. Gln 162 could perform a role in the positioning and stabilization of His 274. Replacement of this group with Asn would increase the distance between the amide functional group and the imidazole ring of histidine and allow this active site catalytic group to occupy additional nonproductive conformations. It has been suggested that asparagine performs a similar role in the catalysis performed by cysteine proteases (*20*), where site-directed mutation of the asparagine to glutamine results in a 3-fold reduction in k_{cat} (*21*). Alternatively, the glutamine could play a role in the orientation of the substrate, as the crystal structure implies by the proximity of the substrate amide group to the amine oxygen of the glutamine. Modeling of the Gln−Asn mutation shows that small adjustments to the position of the substrate analogue allow it to maintain hydrogen bonds with Arg 267 and Glu 241 as observed in the crystal structure as well as a bond with Asn in the place of Gln in position 162. These adjustments would leave the carbon of the substrate less well positioned for catalysis,

which could reduce the k_{cat} with little effect on the K_M as observed experimentally. In either case, the glutamine plays an indirect role in catalysis.

Substrate Binding. The central atoms of the SMCS are identical to the substrate/product, aspartyl phosphate or aspartate semialdehyde. The structure therefore indicates that the substrate α-amino nitrogen interacts with Glu 241 and Gln 162, although mutational results could suggest that the role of Gln 162 in substrate binding is not crucial, as discussed above (*19*). The substrate carboxylate interacts with arginine 267. This arginine corresponds in sequence and spatially with a conserved arginine (Arg 231 in *E. coli*) in glyceraldehyde-3-phosphate dehydrogenase (GAPDH), which is proposed to interact with the phosphate in glyceraldehyde-3-phosphate (*22*). All of these residues that have been identified as having a role in substrate binding are conserved in ASADH across a wide spectrum of species.

Half-of-the-Sites Reactivity. Earlier affinity labeling studies with 2-amino-4-oxo-5-chloropentanoic acid (*23*), a substrate analogue, and an alkylating coenzyme analogue (*24*) each showed a stoichiometry of one molecule of inhibitor incorporated per ASADH dimer. These results were interpreted as supporting a half-of-sites reactivity model for catalysis by ASADH. The absence of electron density for SMCS in subunit B in this complex structure despite its inclusion in the crystallization liquor at a concentration an order of magnitude greater than its inhibition constant with respect to the substrate ASA (0.18 mM) (*6*) is consistent with this interpretation. Since this is a covalent modification there is even a greater likelihood that both sites would be modified over the extended incubation time during crystal growth (3 weeks) if they were equally accessible. It therefore seems likely that structural changes associated with the binding of substrate/inhibitor in one site on the dimer are transmitted to the other site and preclude binding of substrate in the second until the first has turned over, with the enzyme proceeding with an "alternating-sites" mechanism rather than both halves of the dimer working independently.

The asymmetric dimers crystallize with the A and B subunits always in the same orientation with respect to the asymmetric unit, resulting in 100% occupancy of the A site and no occupancy of the B site. This implies that the asymmetry observed in the crystal contacts is due to asymmetry induced by the presence of the SMCS in one of the active sites, since a dimer that was symmetrical (apart from the presence of substrate buried in one active site away from crystal contacts) would presumably be able to pack in either orientation resulting in 50% occupancy of both sites.

The visible differences in conformation between the two subunits are the slight increase in the angle between the N and C terminal domains in the B subunit and the displacement of NADP toward the substrate binding site also in the B (unoccupied) subunit. It is not obvious why these slight changes would result in abrogation of substrate binding in the B subunit. The resolution limit of the current structure makes use of noncrystallographic symmetry restraints in refinement desirable, making subtle differences in conformation of the two subunits difficult to detect. There are two obvious potential routes for transmission of a signal from the active site of one monomer to the other. One is across the dimerization interface. Most of the interactions at this interface are hydrophobic, but there is a buried hydrogen bond between the side chain hydroxyl of Tyr 161 (adjacent to Gln 162 whose side chain is within hydrogen bonding distance of the substrate and Thr 160) and the mainchain of Thr 160 in the opposite subunit, and vice versa. The other involves the "arms" that cross from one subunit to the other at the opposite end of the active site. Arg A173 at one end of helix F is in close contact with the adenine moiety of NADP in subunit A, and residues including Pro A193 and Ser A194 at the other end of helix F are in close contact with the adenine moiety of NADP in subunit B. However, a number of ASADHs including the yeast enzyme have substantial deletions in their sequence which would result in truncation or removal of these arms. If these "arm" subdomains do play a significant role in communication between the subunits of the dimer then the ASADHs that have this domain truncated would be less likely to function by an alternating-site mechanism. Assuming that the mechanism of the enzyme is the same in all cases, this suggests that the arms are not solely responsible for transmission of conformation change from one subunit to the other. A complete structural explanation of this apparent "half of the sites" reactivity phenomenon will have to await a higher resolution structure of an appropriate asymmetric dimer.

Phosphate Binding Site. Examination of the active site also reveals a possible location for the phosphate that is necessary for conversion of aspartate semialdehyde to aspartyl phosphate in the nonphysiological direction (Figure 6). Water molecules are observed in both subunits within hydrogen bonding distance of Arg 102 and Asn 134. Both of these residues are conserved in all of the sequences that are currently available. The site also lies at the N-terminal end of the active site helix. Delphi surface charge calculations reveal that this site is positively charged, while construction of a van der Waals molecular surface reveals a cavity that will accommodate a phosphate group (Figure 6). The positive charge in this binding site is consistent with the observation that high negative charges on the peripheral oxygens of phosphate are essential for binding. Oxyanions with lower charge density on oxygens are either weaker competitive inhibitors or are noninhibitors of ASADH (*25*). This site puts a phosphate oxygen in an appropriate position for attack on the Cγ of the substrate in the reaction in the reverse direction. The equivalent location has also been proposed for the binding site of the attacking phosphate in the mechanism of conversion of glyceraldehyde-3-phosphate to 1,3-bisphosphoglycerate by glyceraldehyde-3-phosphate dehydrogenase (*26*). In this case, the liganding side chains are proposed to be a conserved serine and threonine. A recent structure of the hemiacetal intermediate of GAPDH from *E. coli* revealed the 3-phosphate bound in this cavity rather than the 1-phosphate (*27*). However, this structure was obtained in the absence of the cofactor, NAD, and the proposed binding site for the 3-phosphate, which includes an interaction with the nicotinamide ribose 2′ hydroxyl, was therefore not fully formed. The conformation observed does not allow for acid/base catalysis by His 176, the functional equivalent of His 274 in ASADH. Both the results of kinetics studies on site-directed mutants and the conserved nature of this residue among GAPDH sequences suggest that the histidine plays an important part of the catalysis by GAPDH. It is therefore likely that this hemiacetal intermediate is bound in a nonproductive conformation.

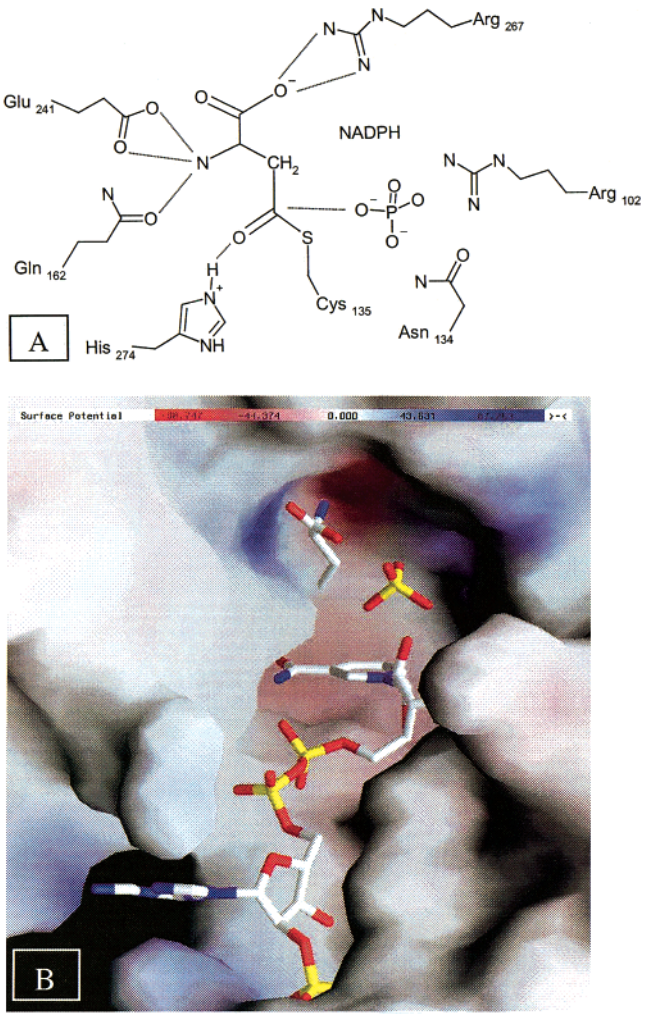

FIGURE 6: (A) Schematic drawing of the thioester intermediate, and phosphate positioned ready for attack, based on the substrate analogue structure. (B) van der Waals surface of ASADH in the vicinity of the active site, colored by electrostatic potential (GRASP). The thioester intermediate, phosphate, and NADP are shown in the active site cleft in bonds representation.

NADP Binding. Experiments conducted before the structure was solved identified Arg 31 and Gln 39 as residues which might be involved in binding the 2′ phosphate moiety of NADP, after sequence comparison with GAPDH (*19*). Substitution of Gln 39 for aspartate resulted in a 10-fold reduction in K_M for NADP. This glutamine is located on the "phosphate binding loop" immediately after residues 36−38 which are polar residues that all appear to be involved in hydrogen bonding interactions with the 2′ phosphate. The end of the side chain lies approximately 5 Å away from the nearest phosphate oxygens. The side chain amine oxygen forms a hydrogen bond with Arg 10. The structure suggests two possible explanations for a decrease in K_M upon substitution of glutamine for the shorter aspartate. This substitution changes the electrostatic environment of the phosphate binding site, introducing a negative charge into the vicinity of the phosphate, which is itself electronegative. The substitution is also likely to affect the conformation of Arg 10. Formation of a salt bridge between this arginine and the shorter aspartate would disrupt the stacking between Arg 10 and the NADP adenine base and probably move the arginine beyond hydrogen bonding distance with the 2′ phosphate. Either or both of these effects would lead to a reduction in K_M for NADP.

Recent alignments of >70 ASADH sequences suggest that Arg 31 is not conserved. NAD binding folds typically have an aspartate at this position in the nucleotide binding domain sequence (*28*), which corresponds structurally to the C-terminal end of the second β-strand. The observed location of this arginine in the ASADH structure is at the opposite, N-terminal, end of the second β-strand in the cofactor binding domain, extending into solvent. The distance between the tip of the arginine side chain and the 2′ phosphate in the bound NADP is approximately 20 Å. This is consistent with the observation that the kinetic parameters for a mutant enzyme with leucine in this position are unchanged from wildtype, although the substitution of a hydrophobic residue in the highly solvent accessible position is likely to lead to some conformational instability.

REFERENCES

1. Cohen, G. N. (1983) in *Amino Acids: Biosynthesis and Genetic Regulation* (Herrmann, K. M., and Somerville, R. L., Eds.) pp 166−171, Addison-Wesley Publishing Company, Reading, MA.
2. Galan, J. E., Nakayama, K., and Curtiss, R. (1990) *Gene 94*, 29−35.
3. Cardineau, G., and Curtiss R. (1987) *J. Biol. Chem. 262*, 3344−3353.
4. Holland, M., and Westhead, E. (1973) *Biochemistry 12*, 2276−2281.
5. Biellmann, J., Eid, P., Hirth, C., and Jornvall, H. (1980) *Eur. J. Biochem. 104*, 53−58.
6. Karsten, W. E., and Viola, R. E. (1991) *Biochim. Biophys. Acta 1077*, 209−219.
7. Hadfield, A. T., Kryger, G., Ouyang, J., Petsko, G. A., Ringe, D., and Viola, R. E. (1999) *J. Mol. Biol. 289*, 991−1002.
8. Segal, H. L., and Boyer, P. D. (1953) *J. Biol. Chem. 204*, 265.
9. Haziza, C., Stragier, P., and Patte, J. (1982) *EMBO J. 1*, 379−384.
10. Preiss, J., Mazelis, M., and Greenberg, E. (1982) *Curr. Microbiol. 7*, 263−268.
11. CCP4. (1994) *Acta Crystallogr. D 50*, 760−763.
12. Brunger, A. T. (1992) *Nature 355*, 472−474.
13. Jones, T. A., Zou, J.-Y., Cowan, S. W., and Kjeldgaard, M. (1991) *Acta Crystallogr. A 47*, 110−119.
14. Brunger, A. T. (1992) Yale University Press, New Haven.
15. Cowtan, K. (1994) *CCP4-ESF-EACBM Newsletter on Protein Crystallography 31*, 34−38.
16. Laskowski, R. A., Macarthur, M. W., Moss, D. S., and Thornton, J. M. (1993) *J. Appl. Crystallogr. 26*, 283−291.
17. Ramachandran, G. N., and Sasisekharan, V. (1968) *Adv. Protein Chem. 28*, 283−437.
18. Karsten, W. E., and Viola, R. E. (1992) *Biochim. Biophys. Acta 1121*, 234−238.
19. Ouyang, J., and Viola, R. E. (1995) *Biochemistry 34*, 6394−6399.
20. Rullmann, J. A. C., Bellido, M. N., and van Duijnen, P. T. (1989) *J. Mol. Biol. 206*, 101−118.
21. Vernet, T., Tessier, D. C., Chatellier, J., Plouffe, C., Lee, T. S., Thomas, D., Storer, A., and Menard, R. (1995) *J. Biol. Chem. 270*, 16645−16652.
22. Asryants, R. A., Kuzminskaya, E. V., Tishkov, V. I., Douzhenkova, I. V., and Nagradova, N. K. (1989) *Biochim. Biophys. Acta 997*, 159−166.
23. Biellmann, J., Eid, P., Hirth, C., and Jornvall, H. (1980) *Eur. J. Biochem. 104*, 59−64.
24. Biellmann, J., Eid, P., and Hirth, C. (1980) *Eur. J. Biochem. 104*, 65−69.
25. Kish, M. M., and Viola, R. E. (1999) *Inorg. Chem. 38*, 818−820.

26. Buehner, M., Ford, G. C., Moras, D., Olsen, K. W., and Rossmann, M. G. (1974) *J. Mol. Biol. 82*, 563−585.
27. Yun, M., Park, C., Kim, J., and Park, H. (2000) *Biochemistry 39*, 10702−10710.
28. Wierenga, R. K., Terpstra, P., and Hol, W. G. (1986) *J. Mol. Biol. 187*, 101−107.

BI015713O